Available online at www.sciencedirect.com
ScienceDirect
Cement and Concrete Research 38 (2008) 40–48
Cement and Concrete Research

# Poroelastic model for concrete exposed to freezing temperatures

Olivier Coussy [a], Paulo J.M. Monteiro [b,*]

[a] Institut Navier, Laboratoire Central des Ponts et Chaussées, France
[b] Department of Civil and Environmental Engineering, University of California at Berkeley, CA 94720, USA

Received 18 August 2006; accepted 13 June 2007

**Abstract**

There are many competing theories to model concrete exposed to freezing temperatures but few of them provide comprehensive quantitative predictions of the mechanical behavior, while accounting for the multi-scale physics of the confined crystallization of ice. When a part of the liquid in the pores solidifies, a pressure build up is generated, and excess liquid is expelled from the freezing sites towards the remaining part of the porous network. In turn, with increasing cooling a cryo-suction process drives the liquid towards the frozen sites. Unsaturated poroelasticity theory provides new perspectives on the computation of stresses and strains developed in such a complex mechanism. The formulation includes the deformation of all the phases during the freezing process. Special attention is given to the influence of entrained air-voids on the frost resistance of the porous material. The analysis indicates that the air voids act both as expansion reservoirs and efficient cryo-pumps whose respective effects are quantitatively assessed. The theory also allows for the estimation of the critical spacing factor. Numerical simulations are conducted to study the effect of pore size distribution on the critical spacing factor and on the internal pressurization within the porous material as it freezes.


*Keywords:* Freezing; Poroelasticity; Cryo-suction; Void; Pore size distribution; Water–cement ratio; Critical spacing factor; Unsaturated

## 1. Introduction

The discovery that a distributed network of small air voids in the cement paste enhanced the frost-resistance of concrete structures was accidental. The demand for a scientific explanation of this important practical observation was temporally met by the development of the hydraulic pressure model by Powers [1]. According to this theory, as the temperature decreases, ice is formed in the cement paste capillaries and, in order to accommodate the volume increase associated with ice formation, excess water is expelled from the freezing sites causing a hydraulic pressure. If the matrix does not have enough tensile strength to resist the resulting pressure, cracks develop and the long-term performance of the structure is compromised. By contrast, air-voids acting as expansion reservoirs can reduce the hydraulic pressure. An important validation of the hydraulic pressure model was the prediction that the critical spacing factor between air-voids should in the order of 250 μ, a value confirmed by laboratory and field work. Subsequent work by Powers and co-workers showed the limitations of the hydraulic model. Powers and Helmuth [2] demonstrated in set of classical experiments that, if a given temperature below freezing is kept constant over a period of time, non-air entrained pastes continue to expand while air-entrained pastes exhibit shrinkage. The hydraulic pressure model alone cannot explain these experimental observations and the authors proposed that the shrinkage was caused by the growth of ice in the air-voids resulting from the diffusion of liquid water from the matrix.

Helmuth further criticized the hydraulic pressure model by pointing out that saturated flows do not occur in the process of freezing mature air-entrained pastes. Instead the accretion of ice in capillaries and air-voids are due to unsaturated flow resulting from suction and surface diffusion [3]. His ideas of crystallization pressure and importance of entrained air-void as a nucleation agent for ice crystallization were expanded by Scherer and Valenza [4].

Even though there are strong criticisms for the hydraulic pressure model (see Chatterji [5] for more details), it is often used and quoted because it is the only major theory capable of providing an order of magnitude of the stress and of the critical

* Corresponding author.
*E-mail address:* monteiro@ce.berkeley.edu (P.J.M. Monteiro).

0008-8846/$ - see front matter © 2007 Published by Elsevier Ltd.
doi:10.1016/j.cemconres.2007.06.006

spacing factor. Yet, as revisited in [6], the original Power s' model considered the paste to be rigid so that it cannot predict the mechanical response of the deformable porous medium depending on the complex interaction between voids, fluid flow, phase transition and the material deformability. Also the hydraulic pressure model predicts the proportionality of the intensity of the hydraulic pressure to the cooling rate, which is against experimental evidence [3].

Since the solidification of water involves a volumetric change, it is important to know how much the matrix deforms to accommodate such expansion. This deformation will affect the magnitude of the resulting hydraulic pressure. Determination of the material deformation is also needed to assess the mechanical role played by entrained air-voids since they act both as expansion reservoirs and cryo-pumps. Therefore a quantitative approach may help establishing the respective mechanical intensity of these effects. The theory may also allow the study of the effect of pore size distribution on the frost resistance of the material and the estimation of the critical spacing factor.

The phase transformation of a fluid inside a porous deformable body can be formulated in the context of poroelasticity originally developed by Biot [7] and expanded in the more general context of continuum thermodynamics by Coussy [8–10]. Poromechanics has proved to be useful to model the mechanical behavior of cement-based materials [11], and has been successfully used to predict the drying shrinkage of these materials [12,13]. This paper extends the fundamental equations needed to model the deformations in concrete exposed to freezing conditions, including hydraulic pressure and cryo-suction, as initially explored in [14], and further developed in [15]. The equations of Poromechanics are then used to study the effect of pore size distribution on the intensity of strain and on the pore pressure build up acting on cement pastes exposed to freezing temperatures. The model allows the identification of the relative importance of air voids acting as expansion reservoir and as a cryo-pump. Finally, the critical spacing factor predicted by this theory is validated with the existing experimental and field results.

## 2. Effect of the pore size distribution on the liquid saturation curve below the melting point

As thoroughly explored in [16], in the context of cement-based materials, the temperature of solidification of water in a given pore depends on the size of the throat which gives access to the pore. This can be shown by first recalling that the solid–liquid thermodynamic equilibrium requires the equality of the chemical potential of both phases. Neglecting both pressure terms of second order with regard to the pressure difference between the crystal pressure $p_C$ and the liquid pressure $p_L$, and temperature terms of second order with regard to the cooling under the melting point, this equality provides

$$p_C - p_L = \Sigma_m (T_m - T), \tag{1}$$

where $T$ is the temperature, while $T_m$ and $\Sigma_m$ are respectively the melting point and the melting entropy. The mechanical equilibrium of the solid–liquid interface with curvature radius $r$ is governed by Laplace law

$$p_C - p_L = \frac{2\gamma_{CL}}{r}, \tag{2}$$

where $\gamma_{CL}$ is the crystal–liquid interface energy. Eqs. (1) and (2) combine to give the celebrated Gibbs-Thomson law:

$$r = \frac{2\gamma_{CL}}{\Sigma_m (T_m - T)}. \tag{3}$$

For the sake of simplicity, we now assume that the angle of contact between the liquid and the solid matrix is zero so that $r$ is also the radius of the pore where the current solid–liquid interface can locate (see for instance [17] for the more general case of a non zero contact angle). As a result it can be inferred from Gibbs–Thomson law (3) that $r$ is the radius of the smallest channels where the ice crystals can propagate when the temperature $T$ is lowered below the melting point $T_m$. Thereby all the pores having an *entry* radius greater than $r$ will freeze at temperature $T$ given by (3).

Standard mercury porosimetry provides the means to determine the cumulative pore volume fraction $1–S(r)$ occupied by pores having a pore entry radius greater than $r$. Using data extracted from the literature [18], the function $1–S(r)$ is illustrated in Fig. 1 for three distinct mortars differing only by their silica fume content. Starting from an initial liquid-saturated cement paste, the volume fraction $S_L$ of the liquid remaining unfrozen at temperature $T$ is finally derived in the form

$$S_L = S\left(r = \frac{2\gamma_{CL}}{\Sigma_m (T_m - T)}\right). \tag{4}$$

Fig. 2 shows the liquid saturation $S_L$ as a function the cooling $\Delta T = T_m - T$ for the three mortars given in Fig. 1. For this determination the following values were used: a zero contact angle and the values $\gamma_{CL} = 0.0409$ J M$^{-2}$ [19], $\Sigma_m = 1.2$ MPa K$^{-1}$ at $T = T_m = 273$ K [20]. It is worth noting that the determination of the $S_L–\Delta T$ curve requires only the knowledge of the cumulative pore volume function $1 - S(r)$ without the need of performing any

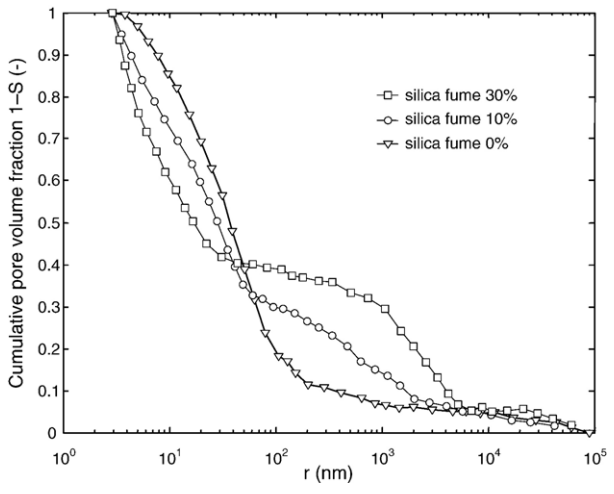


Fig. 1. Cumulative pore volume fraction plotted against pore entry radius for three different mortars. Adapted from [15].

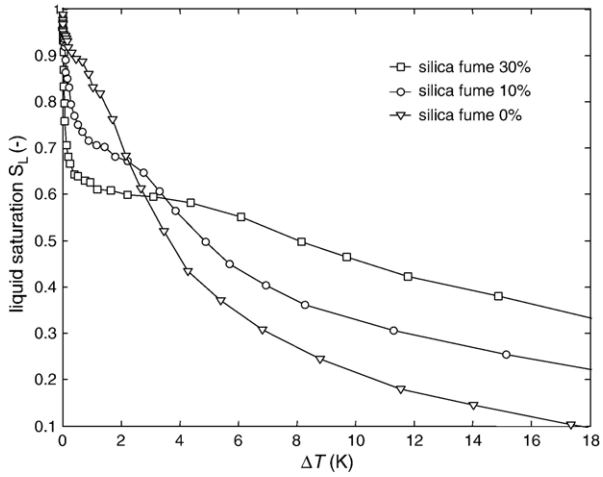


Fig. 2. Liquid saturation $S_L$ plotted against cooling ΔT for the three mortars of Fig. 1.

further freezing test. However, the $S_L$–$\Delta T$. curve can be also determined by a direct experiment, by using for instance dielectric measurements taking advantage of the important contrast in the dielectric constant of liquid water compared with that of ice. This has been done in [21] where the experimental results have been shown to compare well to prediction (4).

Based upon the $S_L$–$\Delta T$ curve, a material characteristic cooling temperature $T_{\rm ch}=T_m-(\Delta T)_{\rm ch}$ can be introduced by weighting the cooling $\Delta T$ with the number of pores whose entry radius $r$ is associated with $\Delta T$ through Gibbs–Thomson law (3). This definition leads to express $(\Delta T)_{\rm ch}$ in the form

$$(\Delta T)_{\rm ch}=\int_{S=0}^{S=1}\Delta T(r)\times dS(r). \tag{5}$$

When using this definition, the values of the characteristic cooling temperature $T_{\rm ch}=T_m-(\Delta T)_{\rm ch}$ are found to be −6 °C, −10 °C and −13 °C associated with the mortars of Figs. 1 and 2 containing respectively 0%, 10% and 30% of silica fume. For $\Delta T\ll\Delta T_{\rm ch}$ a major fraction of water will remain in liquid form while, for $\Delta T\gg\Delta T_{\rm ch}$ almost all water will have solidified.

## 3. Unsaturated poroelasticity for freezing materials

The previous section provided the means of determining the fraction of the porous volume which is frozen at a temperature below the melting point. The purpose of this section is to develop the constitutive equations capable of accounting for the complex mechanical behavior of concrete subjected to freezing. When subjected to freezing, a cement paste deforms as a result of the pore pressure build up caused by the liquid–solid transition. As analyzed in the previous section, because of the combined effect of confinement and surface energy, the liquid saturation of a freezing porous material depends on the current temperature. Accordingly the mechanical behavior of freezing porous materials can be approached through the extension of saturated poroelasticity to unsaturated conditions, where the porous space is filled by two distinct phases, the liquid solution and the solid crystals. In view of such an extension let us first recall the constitutive equations of saturated linear poroelasticity [10,22].

Consider a representative volume $D\Omega_0$ extracted from a porous body. This representative volume has an initial porosity $\varphi_0$ and its initial temperature is the melting temperature $T_m$. The porous body is then further subjected to the cooling $\Delta T=T_m\ T$. Adopting the atmospheric pressure as (zero) reference pore pressure, while assuming a linear isotropic behavior, the constitutive equations of a thermoelastic porous solid whose porous volume is subjected to the uniform pore pressure $p$ are

$$\begin{aligned}&\sigma=K\varepsilon-bp+3aK\Delta T;\\&s_{ij}=2Ge_{ij};\\&\varphi=\phi-\phi_0=b\varepsilon+p/N+\alpha_\phi\Delta T,\end{aligned} \tag{6}$$

where $\sigma$ and $\varepsilon$ are respectively the mean stress and the volumetric dilation; $s_{ij}$ and $e_{ij}$ the components of the deviatoric stress and the deviatoric strain tensors; $K$, $G$ and $a$ are respectively the bulk modulus, the shear modulus and the thermal volumetric dilation coefficient of the porous solid, that are the properties related to the empty porous material with a zero pore pressure; $b$ and $N$ are respectively the Biot coefficient and the Biot modulus. These macroscopic properties are linked to the bulk modulus $k_{\rm s}$ and the thermal volumetric dilation coefficient $\alpha_s$ of the solid matrix according to the relations [10]

$$b=1-\frac{K}{k_s};\ \frac{1}{N}=\frac{b-\phi_0}{k_s};\ a=\alpha_s;\ a_\phi=\alpha_s(b-\phi_0). \tag{7}$$

In the case of a freezing water-infiltrated porous material subjected to a temperature below 0 °C, the pore pressure is no longer uniform since the porous space is partly occupied by ice crystals at pressure $p_{\rm C}$, and partly occupied by the water remaining in liquid form at pressure $p_{\rm L}$. Constitutive Eq. (6) are then extended in the form [10,22]

$$\begin{aligned}&\sigma=K\varepsilon-b_Cp_C-b_Lp_L+3aK\Delta T;\\&s_{ij}=2Ge_{ij};\\&\varphi_C=b_C\varepsilon+p_C/N_{\rm CC}+p_L/N_{\rm CL}+a_C\Delta T;\\&\varphi_L=b_L\varepsilon+p_C/N_{\rm CL}+p_L/N_{\rm LL}+a_L\Delta T.\end{aligned} \tag{8}$$

As $\varphi{\rm d}\Omega_0$ represented in (6) the change undergone by the volume $\phi_0{\rm d}\Omega_0$ under the action of the pore pressure $p$, $\varphi_C{\rm d}\Omega_0$ (resp. $\varphi_L{\rm d}\Omega_0$) represents in (8) the change undergone by the volume $\phi_0S_{\rm C}{\rm d}\Omega_0$ (resp. $\phi_0S_L{\rm d}\Omega_0$) under the action of the crystal pressure $p_C$ (resp. the liquid pressure $p_L$). For its part the overall volume currently occupied by ice crystals (resp. the liquid water) is $\phi_{\rm C}{\rm d}\Omega_0$ (resp. $\phi_L{\rm d}\Omega_0$) with

$$\phi_C=\phi_0S_C+\varphi_C({\rm resp.}\phi_L=\phi_0S_L+\varphi_L), \tag{9}$$

where $S_{\rm J}$ is the current saturation related to phase $J$ with

$$S_C+S_L=1. \tag{10}$$

In (8) coefficients $b_{\rm L}$ and $b_{\rm C}$ are the generalized Biot coefficients related to the liquid and to the solid crystals respectively; $N_{JK}$ are the generalized Biot coupling moduli satisfying the Maxwell symmetry relations $N_{\rm CL}=N_{\rm LC}$, as

anticipated in (8); $a_L$ and $a_C$ are the coefficients related to the thermal volumetric dilation of the pore volume occupied by the liquid and the ice crystals respectively. Micro-macro relations (7) extend in the form (see Appendix)

$$b_C + b_L = b = 1 - \frac{K}{k_s};\ \frac{1}{N_{JJ}} + \frac{1}{N_{\mathrm{LC}}} = \frac{b_J - \phi_0 S_J}{k_s};\qquad (11)$$
$$a_J = \alpha_s(b_J - \phi_0 S_J).$$

Unsaturated poroelastic properties $b_J$ and $N_{JK}$ are current properties depending on the current saturation degree $S_J$. In contrast to relations (9), which are quite general, the missing relations that allows to express $b_J$ and $N_{JK}$ from the knowledge of $S_J$, $\varphi_0$ and the solid matrix properties, depend on the specific morphology of the porous space. Assuming that all pores deform the same when they are subjected to the same pore pressure, Biot coefficient $b_J$ can be expressed in the simple form (see [23] and Appendix)

$$b_J = bS_J, \qquad (12)$$

where $b$ is the Biot coefficient related to the porous solid as defined by (6).

## 4. Development of strain during freezing

Experimental studies of length changes of cement paste and concrete samples exposed to low temperatures are traditionally conducted without application of external load. Under this stress-free condition $\sigma = 0$, the solid–liquid equilibrium condition (1), the first of constitutive Eq. (8) and relations (11) combine to give the volumetric dilation in the form

$$\varepsilon = \frac{bp_L + (b_C\Sigma_m - 3\alpha_s K)\Delta T}{K}. \qquad (13)$$

The determination of $\varepsilon$ requires the determination of $p_L$. To this purpose we will assume that the pores are fully saturated by liquid water before the porous material is exposed to low temperatures. We will also assume that the sample is sealed, so that the total mass of water it contains both in solid and liquid form remains constant during the freezing process. We choose these modeling conditions because they are the ones prevailing in the experiment performed by Beaudoin and MacInnis in [24]. Interestingly, in this experiment the saturating liquid was benzene, which unlike water contracts when it solidifies. In spite of the liquid–solid phase contraction of benzene, Beaudoin and MacInnis have still observed a slight dilation of the sample when they subjected it to freezing. This unexpected phenomenon has to be reproduced by the modeling.

The current mass densities $\rho_C$ and $\rho_L$ of the crystal and liquid are linked to the pressure $p_C$ and $p_L$, and to the current cooling $\Delta T$ through the linearized constitutive equation

$$\frac{1}{\rho_C} = \frac{1}{\rho_C^0}\left(1 - \frac{p_C}{K_C} - 3\alpha_C\Delta T\right) \qquad (14)$$

and

$$\frac{1}{\rho_L} = \frac{1}{\rho_L^0}\left(1 - \frac{p_L}{K_L} - 3\alpha_L\Delta T\right) \qquad (15)$$

where $K_C$ and $K_L$, $\alpha_C$ and $\alpha_L$ are respectively the bulk modulus and the thermal volumetric dilation coefficient of crystal and liquid. Consistently with (9), the total mass of water $m_W$ currently contained in the porous material per unit of initial volume $d\Omega_0$ in both liquid and solid form is

$$m_W = \rho_C(\phi_0 S_C + \varphi_C) + \rho_L(\phi_0 S_L + \varphi_L). \qquad (16)$$

Substituting the poroelastic constitutive equations both for crystal and liquid (8), (14) and (15) into (16), we get

$$m_W = \rho_L^0\phi_0 + \rho_L^0\left(v_{\Delta\rho} + v_\varphi\right), \qquad (17)$$

where

$$v_{\Delta\rho} = \left(\frac{\rho_C^0}{\rho_L^0} - 1\right)\phi_0 S_C \qquad (18)$$

and

$$v_\varphi = b\varepsilon + \frac{p_L}{M_L} + \frac{p_C}{M_C} + 3(\phi_0 S_L\alpha_L + \phi_0 S_C\alpha_C + a_L + a_C)\Delta T, \qquad (19)$$

while $M_J$ is defined by

$$\frac{1}{M_J} = \frac{1}{N_{JJ}} + \frac{1}{N_{\mathrm{LC}}} + \frac{\phi_0 S_J}{K_J}. \qquad (20)$$

The term $v_{\Delta\rho}$ captures the pore volume change due to the change in saturation $S_J$ under the sole condition (10) and to the mass density difference between the two constituents. The term $v_\varphi$ captures the pore volume change due to the thermo-mechanical loading in unsaturated conditions. At this stage of computation the above expressions hold irrespective of the nature of the constituents and, thereby, of the liquid–crystal phase transformation. In other words the expressions of $v_{\Delta\rho}$ and $v_\varphi$ would be the same whatever the constituent $J$ occupying the volume $\phi_0 S_J d\Omega_0$ actually is.

We now specify the approach to freezing porous materials. Using the liquid–crystal equilibrium condition (1), we first get

$$v_\varphi = b\varepsilon + \frac{p_L}{M} + \frac{\Sigma_m}{M_C}\Delta T + 3\left(\sum_{J=L,C}\phi_0 S_J\alpha_J + a_C + a_L\right)\Delta T, \qquad (21)$$

where $1/M = 1/M_C + 1/M_L$. Use of (10), (11) and (20) provides the expression

$$\frac{1}{M} = \frac{1}{N} + \phi_0\left(\frac{S_C}{K_C} + \frac{S_L}{K_L}\right). \qquad (22)$$

Since the liquid is not allowed to escape from the sealed freezing sample, the total mass $m_W$ remains constantly equal to the initial water mass ${\rho_L}^0\phi_0$ so that

$$v_{\Delta\rho} + v_\varphi = 0. \qquad (23)$$

Substitution of (18) and (21) in (23) provides an equation linking $\varepsilon$ and $p_L$. Eliminating $p_L$ between the latter and (13), while using (11) we get

$$\varepsilon = \varepsilon_{th} + \varepsilon_{\Delta\rho} + \varepsilon_{\Sigma_m}, \tag{24}$$

where

$$\varepsilon_{th} = -3\left[\alpha_s + \frac{\phi_0 bM}{K_u}(S_C\alpha_C + S_L\alpha_L - \alpha_s)\right]\Delta T; \tag{25}$$

$$\varepsilon_{\Delta\rho} = \frac{\phi_0 bM}{K_u} S_C\left(1 - \frac{\rho_C^0}{\rho_L^0}\right); \tag{26}$$

$$\varepsilon_{\Sigma_m} = \frac{M}{K_u}\left(\frac{b_C}{M_L} - \frac{b_L}{M_C}\right)\Sigma_m \Delta T, \tag{27}$$

where $K_u = K + b^2 M$. Interestingly, because of (22) $K_u$ represents the bulk modulus of a sealed porous material whose pores would be saturated by a fictitious fluid having $1/(S_L/K_L + S_C/K_C)$ as bulk modulus.

Eq. (24) indicates that the volumetric expansion of a porous material exposed to freezing temperatures is composed of three terms. The term $<\rho_L^0)$ between liquid water and ice crystals. It can be associated to the strain proposed by Power's hydraulic pressure model. Finally the term $\varepsilon_{\Sigma_m}$ indicates the contribution due to a micro-cryo-suction process. Actually, this term would vanish with the melting entropy $\Sigma_m$. With a non zero melting entropy, liquid water has to flow from the still unfrozen part to the frozen sites, in order to meet the liquid–solid equilibrium condition (1), resulting in the contribution $\varepsilon_{\Sigma_m}$ when the thermodynamic equilibrium is finally reached. Its general expression (27) can be made more specific when using the iso-deformation assumption of all pores, allowing us to use (12). Combining (12), (20) and (27) we finally get

$$\varepsilon_{\Sigma_m} = \frac{\phi_0 Mb}{K_u} S_C S_L\left(\frac{1}{K_L} - \frac{1}{K_C}\right)\Sigma_m \Delta T. \tag{28}$$

Since generally $K_C > K_L$ ($K_L \simeq 1.79\times10^3$ MPa at 263 K for supercooled water [25], and $K_C = 7.81\times10^3$ MPa at 263 K for ice crystal [26]), the term $\varepsilon_{\Sigma_m}$ is always positive, even for liquids that usually contract when they solidify. This explain the dilation still observed in [21] in an experiment using benzene as saturating liquid. However, as observed this dilation remains slight owing to the factor $S_C S_L$ involved in (28).

In order to determine the order of magnitude of the three contributions let us now complete the required data. For mortar samples a recent direct experimental estimation of $K$ and $k_s$ has provided the values $K = 17{,}700$ MPa and $k_s = 42{,}400$ MPa [27]. Accordingly, the first relation in (7) gives $b = 0.58$. This value agrees fairly well with the order of magnitude of a previous independent estimation of $b$ to be in the range of 0.48 to 0.54, obtained by combining nano-indentation experiments and uspcaling procedures [28]. We will adopt this value in the forthcoming applications, together with $\varphi_0 = 0.34$ for the initial porosity. The values adopted for the various thermal dilation coefficients are $\alpha_s = 18\times10^{-6}\,K^{-1}$ [29], $3\alpha_L = -286.3\times10^{-6}\,K^{-1}$ at 263 K for supercooled water [25], $3\alpha_C = 155\times10^{-6}\,K^{-1}$ at 263 K for ice crystals [26].

Fig. 3 shows separately the three individual contributions, are close to that of $\varepsilon_{\Delta\rho}$ found to be the leading contribution. The high values of $\varepsilon_{\Delta\rho}$ shown in Fig. 3 must be considered with care since the sample was assumed to be both sealed and initially liquid-saturated. These conditions enhance drastically the volumetric dilation $\varepsilon_{\Delta\rho}$ due to the hydraulic effect because the excess of liquid water expelled from the freezing sites cannot escape from the sample. The values of pressure build up $p_L$ predicted in Fig. 4 from the substitution of $\varepsilon$ in (13) for the three mortars of Figs. 1 and 2 are unrealistically high and the mortars would crack in the first exposure to low temperatures. It should be noted that in Powers' model, the cement paste matrix is assumed to be rigid so the stresses developed during freezing of non-air entrained paste become infinite. This large damage is not observed in field conditions because cement paste and concrete are seldom in fully saturated conditions. The unsaturated zones can decrease the pressure build up during freezing, yet not as efficiently as air-voids as quantified in the next section. This highlight the importance of the experimentally determine the critical degree of saturation and the actual degree of saturation of concrete [28].

Since there is almost one order of magnitude between $\varepsilon_{\Delta\rho}$ and the two other contributions $\varepsilon_{th}$ and $\varepsilon_{\Sigma_m}$ as the cooling $\Delta T$ reaches 18 °C, and owing to the slight difference between the liquid pressure $p_L$ and the crystal pressure $p_C$ induced by cryo-suction (see Fig. 4), it is likely that the hydraulic contribution will generally remain the most important contribution to the overall volumetric dilation in the absence of air-entrained voids, whatever the initial saturation conditions.

The effect of the pore size distribution is shown in Fig. 5 where the overall volumetric strain $\varepsilon$, given by (24), is plotted as a function of cooling $\Delta T$ for the three mortars of Figs. 1 and 2. Since the main contribution to the volumetric strain is $\varepsilon_{\Delta\rho}$, which, according to (26), is proportional to $S_C = 1 - S_L$, the

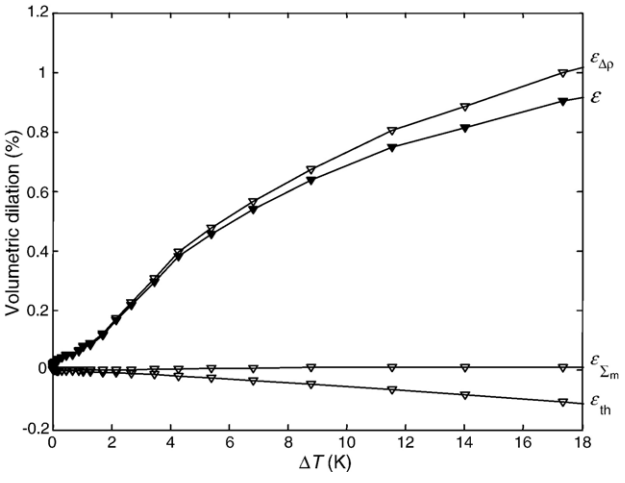


Fig. 3. The three contributions to the volumetric dilation undergone during freezing for the reference mortar with no silica fume of Figs. 1 and 2.

overall volumetric strain as a function of cooling $\Delta T$ reflects faithfully the $S_L-\Delta T$ curves we obtained in Fig. 2 from the pore size distributions of Fig. 1.

## 5. Effect of air-entrained voids

According to the analysis of the previous section, the liquid pore pressure generated during freezing can be severe for intense cooling and can damage significantly the material. Air-entrained voids have been successfully used to prevent such damage. This section describes how the equations of poroelasticity can be used to study the effect of entrained air-voids that when properly distributed in a saturated freezing porous solid act as expansion reservoirs and can accommodate the liquid water expelled from the freezing sites. Originally, the pressure in the air voids is atmospheric and the liquid pressure is zero in the void. Once equilibrium is restored the liquid pressure $p_L$ is zero everywhere so that everywhere the crystal pressure is $p_C=\Sigma_m\Delta T$ according to the thermodynamic equilibrium condition (1). Substituting these values in the first of constitutive Eq. (8) where we let $\sigma=0$, we get

$$\varepsilon\big|_{p_L(R)=0}=\frac{b_C\Sigma_m}{K}-\frac{3\alpha_s K\Delta T}{K}. \tag{29}$$

where $R$ stands for the void radius. In Fig. 5 the curves labeled $p_L(R)=0$ account for the predictions of Eq. (29). They show that the presence of air voids lead to a dramatic reduction in volumetric strain. In fact, in the presence of air voids the three previous mortars are even predicted to shrink. The presence of air voids prevent the hydraulic effect to happen so that the only expansive effect is due to the crystal pressure $p_C=\Sigma_m\Delta T$. The comparison of the thermal contribution given in Fig. 3 for the reference mortar, with the shrinkage obtained in Fig. 4 in the presence of air voids, show that we are mainly left with the thermal shrinkage in the latter case.

Besides acting as an expansion reservoir, the air-voids perform as a cryo-pump. Since the pressure in the air void is atmospheric, the liquid water expelled from the freezing sites freezes when

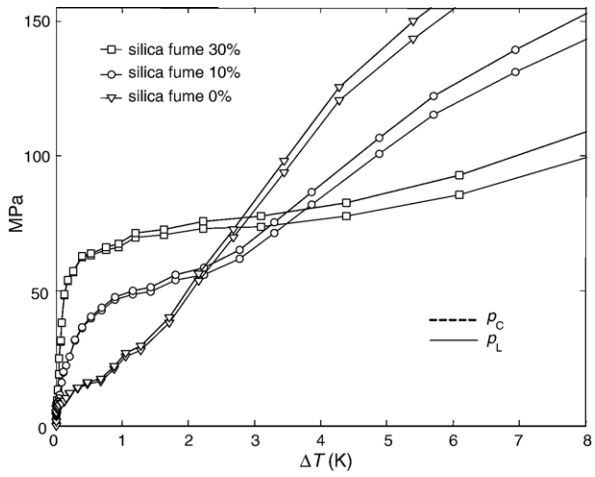


Fig. 4. Liquid pressure build up $p_L$ and crystal pressure $p_C$ predicted for the three mortars of Figs. 1 and 2 in the absence of air-entrained voids.

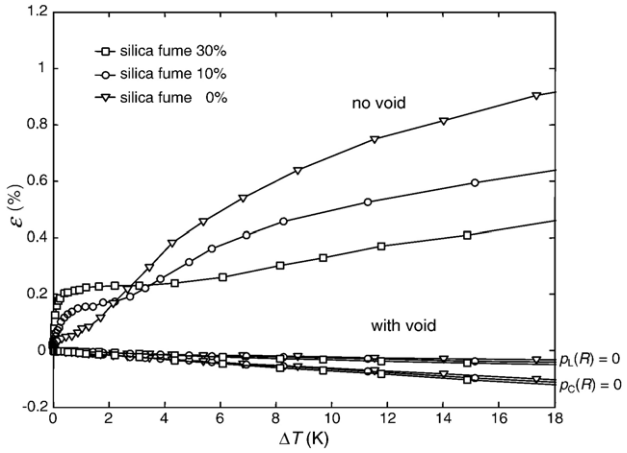


Fig. 5. Volumetric dilation undergone during freezing predicted for the three mortars of Figs. 1 and 2 in the absence of air-entrained voids (upper curves) and with air-entrained voids (lower curves). For the latter case the curve labeled $p_L(R)=0$ accounts for the air void acting only as an expansion reservoir, while the curve labeled $p_C(R)=0$ accounts for the air void acting both as an expansion reservoir and as a cryo-pump.

entering the air void. As long there is space for ice crystals to form in an air void, the pressure of these crystals remains atmospheric. As a result, according to (1) the pressure of the liquid in contact with the crystals, instead of being zero as assumed in (29), is equal to $p_L=-\Sigma_m\Delta T$. Substitution of $p_L=-\Sigma_m\Delta T$ and $p_C=0$ in the first of constitutive Eq. (8) gives

$$\varepsilon\big|_{p_C(R)=0}=-\frac{b_L\Sigma_m}{K}-\frac{3\alpha_s K\Delta T}{K}. \tag{30}$$

In Fig. 5 the curves labeled $p_C(R)=0$ account for the prediction of Eq. (30). The added cryo-pump effect played by the air void enhances the shrinkage. Actually, as previously analyzed in [4] and [15], in order to continuously restore everywhere the equilibrium condition (1) with $p_C=0$, some extra water has to be sucked towards the air void resulting in an extra shrinkage. This extra shrinkage has been directly observed in [30].

Predictions from Eqs. (29) and (30) are equilibrium values. They correspond to infinitely slow cooling rates with regard to the rate of the liquid flow towards the air void achieving the equilibrium. The effect of non infinitely slow cooling rates has been explored in [15], which a special attention being given in [6] to the air void transition layer. Here we will restrict ourselves to determine the validity range of assuming infinitely slow cooling rates. The characteristic time $\tau_{\Delta T}$, scaling the cooling rate with regard to the solidification within a porous material, can be assessed in the form

$$\tau_{\Delta T}=(\Delta T)_{\rm ch}/\overset{o}{\Delta T}, \tag{31}$$

where $(\Delta T)_{\rm ch}$ is the characteristic cooling defined in (5), while $\overset{o}{\Delta T}$ is the imposed cooling rate. The characteristic time $\tau_w$, scaling the hydraulic diffusion of liquid water towards the void, can be expressed in the form

$$\tau_w=\frac{L^2}{4D}, \tag{32}$$

where $L$ is the spacing factor, the distance between the centers of two neighboring spherical voids of radius $R$ being equal to $2R+L$. The expression of the hydraulic diffusivity $D$ is [10]

$$D=\frac{\kappa}{\eta_L}\Big/\left(\frac{b^2(1+\nu)}{3K(1-\nu)}+\frac{\phi_0}{K_L}+\frac{b-\phi_0}{k_s}\right), \tag{33}$$

where $\nu$ is the Poisson coefficient of the porous solid and $\kappa$, its intrinsic permeability, while $\eta_L$ ($\simeq 1.79\times10^{-3}$ Pa s at 273 K [26,31]) is the liquid water viscosity. Cooling rates can be considered as infinitely slow with regard to the liquid flow if $\tau_w \ll \tau_{\Delta T}$, providing the condition

$$L^2 \ll 4D\times(\Delta T)_{ch}\Big/\overset{o}{\Delta T}. \tag{34}$$

In practice, according to [29] the order of magnitude of *in situ* cooling rates does not exceed a few $K\cdot h^{-1}$ and, in order to explore condition (34), we adopt the value $\overset{o}{\Delta T}=3K\cdot h^{-1}$. For the three mortars analyzed above, we found that the order of magnitude of $(\Delta T)_{ch}$ was 10 K. If we adopt $\nu=0.3$ and the poroelastic properties reported above, the hydraulic diffusivity takes the form

$$D\left(m^2\cdot s^{-1}\right)=2.710^{12}\times\kappa\left(m^2\right). \tag{35}$$

Use of these data in (34) provides the condition

$$L^2\left(m^2\right)\ll 1.310^{17}\times\kappa\left(m^2\right). \tag{36}$$

The order of magnitude of the lowest values of the intrinsic permeability of high strength mortars is $\kappa\simeq 10^{-21}$ ($m^2$) (see for instance [32,33]). Even for these extreme permeability values, the condition (36) is not restrictive. Actually (36) provides the conditions L « 1 cm and the upper bond values of the spacing factor experimentally observed to prevent internal damage are of millimeter order [34]. As a result predictions (29) and (30) are relevant with regard to *in situ* cooling rates, whereas (36) does not provide any actual restriction concerning the critical spacing factor.

## 6. Critical spacing factor

As pointed out in [4], air-entrained voids likely play the role of nucleation agents. This nucleation role is critical to support predictions (29) and (30) since it limits the supercooling of water and, thereby, ensures with (36) that the thermodynamical equilibrium captured by $S_L$–$\Delta T$ curves is likely achieved at any stage of the freezing process. However, although important, this role is non-mechanical and does not quantitatively affect (29) and (30). According to the above analysis of the previous sections, the main mechanical effect of air-entrained voids remains their capability to welcome the liquid water expelled from the freezing site. As discussed in the previous section, the mechanical effect of air-entrained voids acting as cryo-pumps has been found to be an order of magnitude smaller than the expansion reservoir effect (see Fig. 5).

Restricting to the mechanical effects, the right choice of the spacing factor $L$ has finally to meet the condition that the void must be large enough in order to avoid any in-void pressure build up. In order to be on the safe side we may disregard the ability of unsaturated zones to accommodate the extra liquid water. The corresponding condition has then to express that the void volume $4\pi R^3/3$ is capable to welcome the totality of the liquid water expelled from the adjacent freezing sites owing to the ice-liquid difference of density. The zone of influence of a void is the spherical shell, with inner radius $R$ and outer radius $R+L/2$. Its volume is $V_{shell}=(4\pi/3)[(R+L/2)^3-R^3]$. At equilibrium related to cooling $\Delta T$ the volume of liquid that has frozen within this shell is $V_{L\to C}=\phi_0[1-S_L(\Delta T)]\times V_{shell}$, where $S_L(\Delta T)$ is given by the $S_L$–$\Delta T$ curve. During solidification the volume change is $(\rho_L^0/\rho_C^0-1)\times V_{L\to C}$. As a result there will be no pressure build up within the void if the following relation is satisfied

$$\left(\frac{\rho_L^0}{\rho_C^0}-1\right)\times\phi_0[1-S_L(\Delta T)]\times\frac{4\pi}{3}\left[\left(R+\frac{L}{2}\right)^3-R^3\right]<\frac{4\pi}{3}R^3. \tag{37}$$

Fig. 6 shows the normalized ratio $L/R$ as a function of $\Delta T$ for the three mortars whose $S_L$–$\Delta T$ curve is given in Fig. 2. The values of the ratio $L/R$ reported in Fig. 5 agree with the order of magnitude of the experimental values [34] known to preserve the cement-based materials from bulk damage under freezing. For instance, adopting $R=50$ μm the results shown up in Fig. 5 provides the value $L=250$ μm as a safe choice for the three mortars down to $T=-12$ °C.

## 7. Conclusions

Internal damage due the frost action can nowadays be avoided by the help of air-entrained voids and by adopting a spacing factor in agreement with experimental data and good practice. There was a lack of a comprehensive model that could compare the effects of the hydraulic pressure, cryo-suction, and

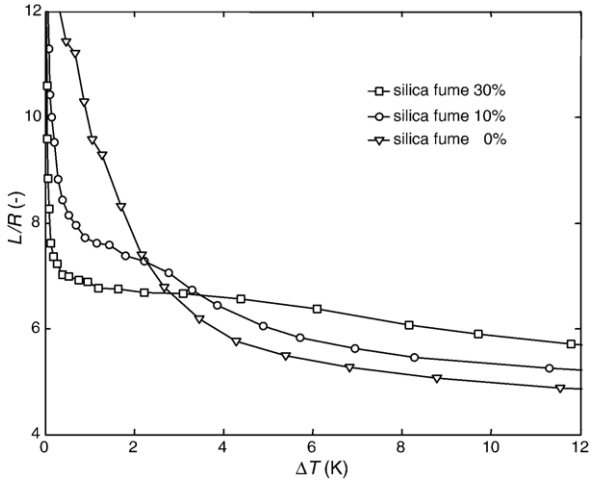


Fig. 6. Critical spacing factor plotted against cooling for the three mortars of Figs. 1 and 2.

thermal mismatch of the constituents on the performance of concrete exposed to low temperatures. Also classical models did not include the deformation of the solid matrix during freezing conditions.

Poromechanics has the flexibility to extend Powers hydraulic pressure theory in order to account for the deformation of the matrix and for the development of cryo-suction in air voids. The simulations of the resulting equations using values relevant to concrete exposed to freezing conditions indicate that for saturated conditions the dominant mechanism of concrete expansion is the hydraulic pressure caused by the transformation of liquid water into ice and excess liquid is expelled from the freezing sites. Unlike in Powers model, the stresses developed during freezing of saturated non-air entraining paste are finite. The high values of the predicted stresses reflect the assumption of full saturation of matrix, a condition that may take time to develop in field concrete.

The presence of air-voids can be easily incorporated in the poroelastic equations which can provide quantitative values for the reduction of pressure build up during freezing. The model predicts well the shrinkage experimentally observed in air-entrained pastes during freezing. Due to this shrinkage the stress is no more tensile but compressive in the matrix.

In the original Powers' model, when temperature stops dropping, the deformation has to stop as well whereas the shrinkage observed by Piltner and Monteiro [30] was delayed. This delay can only be explained by hydromechanical coupling, such as the one developed in the present poromechanics model.

The predictions of the model have been validated by obtaining realistic values of the critical factor $L$. A simple methodology is proposed to determine the critical factor $L$: i) determine the cumulative volume fraction as a function of the pore entry radius (see Fig. 1); ii) determine the $S_L$–$\Delta T$ curve from (4) (see Fig. 2); iii) for a given extreme cooling $\Delta T$ determine the upper bond allowable for $L$ from inequality (37) (see Fig. 2). The method is on the safe side with regard to initial conditions in liquid saturation. The method can obviously be refined by accounting for the hysteretic character of the $S_L$–$\Delta T$ curve, and by taking into account that drying shrinkage prior to freezing could significantly affect the cumulative volume fraction as a function of the pore entry radius.

**Acknowledgments**

The authors acknowledge the support for this work of the Berkeley-France funds. Paulo Monteiro wishes to acknowledge the financial support of NSF Grant CMS-0301288.

**Appendix**

In order to derive (11) let us start by letting $p_C=p_L=p$ in the first of Eq. (8). We get

$$\sigma = K\varepsilon - (b_C + b_L)p_L + 3aK\Delta T. \tag{A1}$$

The above equation must be the constitutive equation of a porous solid whose pore pressure is $p$ As a result, a comparison of the first of Eqs. (6) and (A1) provides the first of relations (11). To obtain the remaining equations, let us now recall that the macroscopic stress $\sigma$ is the space averaged of the microscopic stress, that is

$$\sigma = (1-\phi_0)\sigma_S - \phi_0 S_C p_C - \phi_0 S_L p_L, \tag{A2}$$

where $\sigma_S$ stands for the averaged mean stress within the solid matrix. Furthermore let us consider an experiment where

$$\sigma = -p;\ p_C = p_L = p;\ \Delta T = 0. \tag{A3}$$

A combination of (10) and the two last equations provides

$$\sigma_S = -p, \tag{A4}$$

so that the volumetric strain $\varepsilon_S$ related to the solid matrix (assumed to be homogeneous) is

$$\varepsilon_S = -p/k_S. \tag{A5}$$

In the particular experiment defined by the loading condition (A3) the porous solid is loaded externally and internally by an uniform pressure on its boundary. Similarly to a spherical shell externally and internally loaded by the same pressure, the volumetric deformation is then uniform within the solid matrix and identifies to the relative change of the pore volume whatever the pore considered. It results in

$$\varepsilon = \varphi_J/\phi_0 S_J = \varepsilon_S. \tag{A6}$$

Substitution of (A6) in (A5) we get

$$\varepsilon = \varphi_J/\phi_0 S_J = -p/k_S. \tag{A7}$$

Eqs. (A5) and (A7) used in the two last equations of (8) finally provides the second of relations (11). The last of relations (11) can be obtained by extending the approach given in [10] to derive in the saturated case the last of relations (7).

Relations (11) are quite general since they do not rely upon any assumption on the porous material (except the isotropy of the porous network and the homogeneity of the porous matrix). However they do not allow the separate determination of poroelastic properties $b_J$ and $N_{JK}$, which depend on the precise geometry of the porous network and on the current saturation degree $S_J$. In order to give an assessment of these properties, let us assume that all pores deform the same when they are subjected to the same pore pressure $p$. Accordingly, we write

$$\left(\frac{\varphi_C}{\phi_0 S_C}\right)_{p_C=p_L=p} = \left(\frac{\varphi_L}{\phi_0 S_L}\right)_{p_C=p_L=p}. \tag{A8}$$

Substitution of (A8) in the two last equations of (8) provides

$$\left(\frac{b_C}{S_C} - \frac{b_L}{S_L}\right)\varepsilon + \left(\frac{1}{S_C}\left(\frac{1}{N_{CC}} + \frac{1}{N_{CL}}\right) - \frac{1}{S_L}\left(\frac{1}{N_{LL}} + \frac{1}{N_{CL}}\right)\right)p + \left(\frac{a_C}{S_C} - \frac{a_L}{S_L}\right)\Delta T = 0. \tag{A9}$$

Since the above equation must hold whatever the values of the independent loading parameters, the factors of $\varepsilon$, $p$ and $\Delta T$ must be zero, resulting in particular in

$$\frac{b_C}{S_C}=\frac{b_L}{S_L};\ \frac{1}{S_C}\left(\frac{1}{N_{CC}}+\frac{1}{N_{CL}}\right)=\frac{1}{S_L}\left(\frac{1}{N_{LL}}+\frac{1}{N_{CL}}\right);\ \frac{a_C}{S_C}=\frac{a_L}{S_L}. \tag{A10}$$

Substitution of the first of relations (A10) in the first of Eqs. (11) provides (12). Use of the two last Eqs. of (11) and (12) show that the two last relations of (A10) are satisfied. It is worth noting that, adding the two last constitutive equations of (8) while taking into account of (12) together with general relations (7), (9) and (11), we get

$$\begin{aligned}&\sigma = K\varepsilon - b(S_C p_C + S_L p_L) + 3aK\Delta T;\\ &s_{ij} = 2Ge_{ij};\\ &\varphi = \varphi_C + \varphi_L = b\varepsilon + (S_C p_C + S_L p_L)/N + \alpha_\phi \Delta T.\end{aligned} \tag{A11}$$

Constitutive Eq. (A11) identify to the standard constitutive Eq. (6) of saturated poroelasticity provided that the pore pressure $p$ is replaced in the later by the averaged pore pressure $S_C p_C + S_L p_L$. It can be then concluded that, under assumption (A8), saturated poroelasticity extends to unsaturated poroelasticity by simply replacing $p$ by $S_C p_C + S_L p_L$. However it must be kept in mind that assumption (A8) that all the pores have the same deformation remains a rough assumption. This holds for pores of same shape in the dilute approximation where the interaction between adjacent pores is negligible. This hold too for pores of same shape and of same size uniformly distributed so that each pore experiences the same interaction with the surrounding pores. The relations obtained up to now are still insufficient for the separate assessment of $N_{JK}$. Fortunately, the approach developed here for the freezing of porous materials does not need the separate determination of $N_{JK}$.

## References


[1] T. Powers, The air requirement of frost-resistant concrete, Highway Research Board, PCA Bulletin 33 (29) (1949) 184–211.

[2] T. Powers, R.A. Helmuth, Theory of volume changes in hardened Portland cement paste during freezing, Proceedings, Highway Research Board, Bulletin no. 33, Portland Cement Association, vol. 32, 1953, pp. 286–297.

[3] R.A. Helmuth, Discussion of the paper "Frost action in concrete", in: P. Nerenst (Ed.), Proceedings of the 4th International Congress on Chemistry of Cement, 1960, pp. 829–833.

[4] G.W. Scherer, J.J. Valenza, in: F. Young, J. Skalny (Eds.), Mechanism of Frost Damage, Materials Science of Concrete VII, American Ceramic Society, 2005.

[5] S. Chatterji, Freezing of air-entrained cement-based materials and specific actions of air-entraining agents, Cement and Concrete Composites 25 (2003) 759–765.

[6] P.J.M. Monteiro, O. Coussy, D. Silva, A. Effect of cryo-suction and air void transition layer on hydraulic pressure of freezing concrete, American Concrete Institute, Materials Journal, ACI 103 (2) (2006) 136–140.

[7] M.A. Biot, General theory of three dimensional consolidation, Journal of Applied Physics 12 (1941) 155–164.

[8] O. Coussy, A general theory of thermoporoelastoplasticity for saturated materials, Transport in Porous Media 4 (1989) 281–293.

[9] O. Coussy, E. Detournay, L. Dormieux, From mixture theories to Biot's theory, International Journal of Solids and Structures 35 (34-35) (1998) 4619–4635.

[10] O. Coussy, Poromechanics, John Wiley and Sons, 2004.

[11] Poromechanics of concrete I and II, Materials and structures/Concrete and Science Engineering, December 2003, and January 2004, O. Coussy, G. Scherer editors.

[12] O. Coussy, R. Eymard, T. Lassabatère, Constitutive modelling of unsaturated drying deformable materials, Journal of Engineering Mechanics, 124 (6) (1998) 658–667.

[13] O. Coussy, P. Dangla, T. Lassabatère, V. Baroghel-Bouny, The Equivalent Pore Pressure and the Swelling and Shrinkage of Cement-Based Materials, Materials and Structures/Concrete and Science Engineering 37 (2004) 15–20 (n° 265).

[14] B. Zuber, J. Marchand, Predicting the volume instability of hydrated cement systems upon freezing using poro-mechanics and local phase equilibria, Materials and Structures/Concrete Science Engineering 37 (268) (2004) 257–270.

[15] O. Coussy, Poromechanics of freezing materials, Journal of the Mechanics and Physics of Solids 53/8 (2005) 1689–1718.

[16] G.W. Scherer, Crystallization in pores, Cement and Concrete Research 29 (1999) 1347–1358.

[17] O. Coussy, P. Monteiro, Unsaturated poroelasticity for crystallization in pores, Computers and Geotechnics 34 (2007) 279–290.

[18] H. Cheng-yi, R.F. Feldman, Dependence of frost resistance on the pore structure of mortar containing silica fume, ACI Journal 82-68 (1985) 740–743.

[19] M. Brun, A.J. Lallemand, F. Quinson, C. Eyraudand, Thermochimica Acta 21 (1977) 59–88.

[20] V.F. Petrenko, R.W. Whitworth, Physics of Ice, 1st edition, Oxford University Press, 1999.

[21] A. Fabbri, T. Fen-Chong, O. Coussy, Dielectric capacity liquid water content, and pore structure of thawing-freezing materials, Cold Regions Science and Technology 44 (2006) 52–66.

[22] O. Coussy, Deformation and stress from in-pore drying-induced crystallization of salt, Journal of the Mechanics and Physics of Solids 54 (2006) 1517–1547.

[23] X. Chateau, L. Dormieux, Micromechanics of saturated and unsaturated porous media, International Journal for Numerical and Analytical Methods in Geomechanics 26 (2002) 831–844.

[24] J.J. Beaudoin, C. MacInnis, The mechanism of frost damage in hardened cement paste, Cement and Concrete Research 4 (1974) 139–147.

[25] R.J. Speedy, Thermodynamic properties of supercooled water at 1 atm, The Journal of Physical Chemistry 91 (1987) 3354–3358.

[26] D.R. Lide, Handbook of Chemistry and Physics 2001-2002, CRC Press, 2001.

[27] Skoczylas, 2006. Personal communication.

[28] P.K. Mehta, P.J.M. Monteiro, Concrete, Structure, Properties, and Materials, 3rd edition, McGraw-Hill, 2006.

[29] J.-F. Ulm, G. Constantinides, F.H. Heukamp, Is concrete a poromechanics material? A multiscale investigation of poroelastic properties, Material and Structures/Concrete Science Engineering 37 (265) (2003) 43–58.

[30] R. Piltner, P. Monteiro, Stress analysis of expansive reactions in concrete, Cement and Concrete research 30 (2000) 843–848.

[31] J. Hallet, The temperature dependance of the viscosity of supercooled water, Proceedings of the Physical Society 82 (1963) 1046–1050.

[32] V. Baroghel-Bouny, M. Mainguy, O. Coussy, Isothermal drying process in weakly permeable cementitious material — assessment of water permeability, in: R.D. Hooton, M.D.A. Thomas, J. Marchand, J.J. Beaudoin (Eds.), Material Science of Concrete, Special Volume: Ion and Mass Transport in Cement Based Materials, Am. Ceram. Soc., Westerville, OH, 2001, pp. 59–80.

[33] M. Mainguy, O. Coussy, V. Baroghel-Bouny, The role of air pressure in the drying of weakly permeable materials, Journal of Engineering Mechanics, ASCE 127 (6) (2001) 582–592.

[34] J. Marchand, M. Pigeon, Résistance du béton à l'écaillage dû au gel en présence de sels fondants: une revue des récents développements dans le domaine (strength of concrete to scaling upon freezing in presence of deicer salts: a review), in: J.P. Bournazel, Y. Malier (Eds.), Proceedings of RILEM Conference "Concrete: from material to structure", Arles, France, 1996.